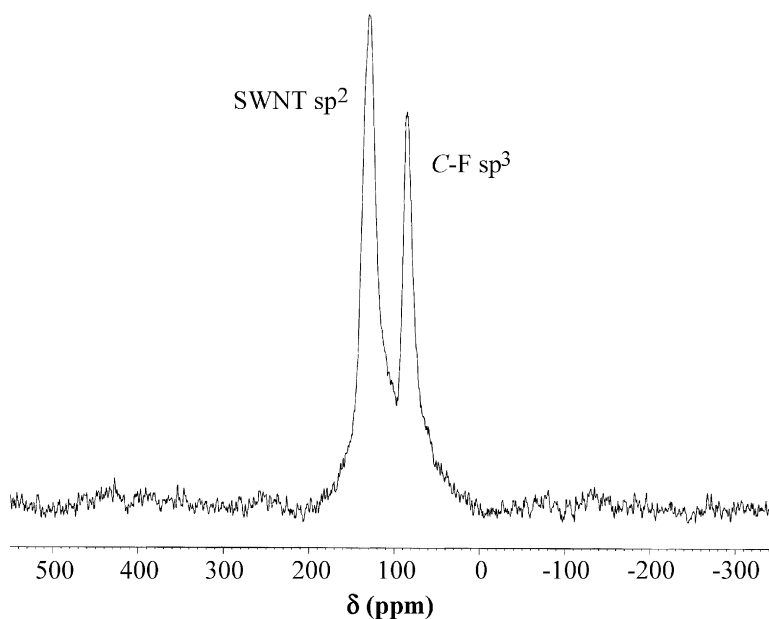


## Solid-State NMR Analysis of Fluorinated Single-Walled Carbon Nanotubes: Assessing the Extent of Fluorination

Lawrence B. Alemany, Lei Zhang, Liling Zeng, Christopher L. Edwards, and Andrew R. Barron

*Chem. Mater.*, **2007**, 19 (4), 735-744 • DOI: 10.1021/cm0618906

Downloaded from <http://pubs.acs.org> on January 13, 2009



### More About This Article

Additional resources and features associated with this article are available within the HTML version:

- Supporting Information
- Links to the 7 articles that cite this article, as of the time of this article download
- Access to high resolution figures
- Links to articles and content related to this article
- Copyright permission to reproduce figures and/or text from this article

[View the Full Text HTML](#)



ACS Publications  
High quality. High impact.

# Solid-State NMR Analysis of Fluorinated Single-Walled Carbon Nanotubes: Assessing the Extent of Fluorination

Lawrence B. Alemany,<sup>†,‡</sup> Lei Zhang,<sup>‡</sup> Liling Zeng,<sup>‡</sup> Christopher L. Edwards,<sup>‡</sup> and Andrew R. Barron<sup>\*,†,‡,§</sup>

Richard E. Smalley Institute for Nanoscale Science and Technology and Departments of Chemistry and of Mechanical Engineering and Materials Science, Rice University, Houston, Texas 77005

Received August 10, 2006. Revised Manuscript Received November 20, 2006

Fluorinated single-walled carbon nanotubes (F-SWNTs) have been characterized by magic angle spinning  $^{13}\text{C}$  NMR spectroscopy and the results correlated with Raman, IR, and X-ray photoelectron spectroscopy measurements. The  $^{13}\text{C}$  NMR shift for the  $\text{sp}^3$  fluorine-substituted (CF) carbon atoms of the SWNT sidewall is observed at  $\delta = 83.5$  ppm. This apparently unusual shift compared to those of most other tertiary alkyl fluorides is confirmed to be due to the CF moieties from ab initio calculations on an 80-carbon fragment of the 5,5 (armchair) SWNT and is in good agreement with the predominance of 1,2-addition rather than 1,4-addition of fluorine. The lack of observable scalar  $^{13}\text{C}$ – $^{19}\text{F}$  coupling for the CF carbon signal over a wide range of spinning speeds and at two different field strengths apparently results from interaction between  $^{19}\text{F}$ – $^{19}\text{F}$  and  $^{13}\text{C}$ – $^{19}\text{F}$  dipolar couplings and from magnetization exchange between the  $^{13}\text{C}$  doublet components caused by fluorine spin diffusion. The assignment of the 83.5 ppm peak is further confirmed by the correlation of its diminished intensity upon thermolysis of the F-SWNT (400, 450, and 550 °C) with the relative intensity of the D (disorder) band in Raman and the C:F ratio from X-ray photoelectron spectroscopy (XPS). On the basis of the XPS signal, it appears that the  $\text{CF}_2$  defect units decompose at a lower temperature than the CF sidewall moieties, suggesting that cutting chemistry precedes sidewall functional group removal. We propose that, where a comparison of samples with a high degree of functionalization is required, NMR provides a much better quantification than Raman. However, where a comparison between samples with low levels of functionalization or large differences in degree of functionalization is required, Raman provides a much better quantification than NMR.

## Introduction

Fluorinated single-walled carbon nanotubes (F-SWNTs)<sup>1–3</sup> offer advantages as a synthon for sidewall-functionalized SWNTs with a wide range of functional groups by the reaction with organolithium and Grignard reagents or primary amines.<sup>4–7</sup> Fluorination is accomplished by the direct reaction of purified SWNTs with  $\text{F}_2$  gas diluted in argon, along with HF (proposed to act as a catalyst).<sup>2,3</sup> A saturation stoichiometry is reached of ca.  $\text{C}_2\text{F}$  without destruction of the tube structure. F-SWNTs are shown to form metastable solutions of individual tubes (as opposed to bundles) in DMF, THF,

and alcohols, and it is these solvents that are most often employed for further functionalization.<sup>4–7</sup> Computational and experimental results are ambiguous as to whether 1,2-addition<sup>8</sup> or 1,4-addition<sup>9</sup> of  $\text{F}_2$  to the sidewall predominates.<sup>10</sup> STM images indicate that fluorination occurs in bands along the length of the tube,<sup>9</sup> however, calculations suggest that addition along the SWNT axis should be preferred over that around the circumference.<sup>10</sup> Irrespective of the arrangement of the F substituents, thermolysis of F-SWNTs results in their cleavage into shorter lengths. For example, fluorination to a formula of  $\text{C}_3\text{F}$  followed by pyrolysis results in the cutting of SWNTs into short lengths (20–100 nm).<sup>11,12</sup>

Unlike typical organic molecules, the characterization of functionalized SWNTs has been accomplished with Raman

\* To whom correspondence should be addressed. E-mail: arb@rice.edu. URL: www.rice.edu/barron.

<sup>†</sup> Richard E. Smalley Institute for Nanoscale Science and Technology.

<sup>‡</sup> Department of Chemistry.

<sup>§</sup> Department of Mechanical Engineering and Materials Science.

- (1) Margrave, J. L.; Mickelson, E. T.; Hauge, R.; Boul, P.; Huffman, C.; Liu, J.; Smalley, R. E.; Smith, K.; Colbert, D. T. U.S. Patent 6,835,366, 2004.
- (2) Mickelson, E. T.; Huffman, C. B.; Rinzler, A. G.; Smalley, R. E.; Hauge, R. H.; Margrave, J. L. *Chem. Phys. Lett.* **1998**, *296*, 188.
- (3) Khabashesku, V. N.; Billups, W. E.; Margrave, J. L. *Acc. Chem. Res.* **2002**, *35*, 1087.
- (4) Boul, P. J.; Liu, J.; Mickelson, E. T.; Huffman, C. B.; Ericson, L. M.; Chiang, I. W.; Smith, K. A.; Colbert, D. T.; Hauge, R. H.; Margrave, J. L.; Smalley, R. E. *Chem. Phys. Lett.* **1999**, *310*, 367.
- (5) Stevens, J. L.; Huang, A. Y.; Peng, H.; Chiang, I. W.; Khabashesku, V. N.; Margrave, J. L. *Nano Lett.* **2003**, *3*, 331.
- (6) Zhang, L.; Zhang, J.; Schmandt, N.; Cratty, J.; Khabashesku, V. N.; Kelly, K. F.; Barron, A. R. *Chem. Commun.* **2005**, 5429.
- (7) Yang, L.; Zhang, L.; Barron, A. R. *Nano Lett.* **2005**, *5*, 2001.

- (8) DFT (PBE/3-21G and LSDA/3-21G) calculations suggest that the 1,2-isomer is more stable by 16.7  $\text{kJ}\cdot\text{mol}^{-1}$ : Kudin, K. N.; Bettinger, H. F.; Scuseria, G. E. *Phys. Rev. B* **2001**, *63*, 45413.
- (9) Molecular mechanics (MM+) and semiempirical (AM1 and CNDO) calculations suggest that the 1,4-isomer is more stable by 4.1  $\text{kJ}\cdot\text{mol}^{-1}$ : Kelly, K. F.; Chiang, I. W.; Mickelson, E. T.; Hauge, R. H.; Margrave, J. L.; Wang, X.; Scuseria, G. E.; Radloff, C.; Halas, N. J. *Chem. Phys. Lett.* **1999**, *313*, 445.
- (10) (a) Park, K. A.; Choi, Y. S.; Lee, Y. H.; Kim, C. *Phys. Rev. B* **2003**, *68*, 045429/1. (b) Pehrsson, P. E.; Zhao, W.; Baldwin, J. W.; Song, C.; Liu, J.; Kooi, S.; Zheng, B. *J. Phys. Chem. B* **2003**, *107*, 5690. (c) Jaffe, R. L. *J. Phys. Chem. B* **2003**, *107*, 10378. (d) Van Lier, G.; Ewels, C. P.; Zuliani, F.; De Vita, A.; Charlier, J.-C. *J. Phys. Chem. B* **2005**, *109*, 6153.
- (11) Gu, Z.; Peng, H.; Hauge, R. H.; Smalley, R. E.; Margrave, J. L. *Nano Lett.* **2002**, *2*, 1009.
- (12) Bettinger, H. F.; Peng, H. *J. Phys. Chem. B* **2005**, *109*, 23218.

and IR spectroscopy, TGA, AFM, and STM. Unfortunately, AFM and TGA do not unambiguously determine whether functional groups are covalently bound rather than absorbed onto the SWNT's surface. The presence of a significant D (disorder) mode at ca.  $1300\text{ cm}^{-1}$  is consistent with sidewall functionalization,<sup>13</sup> and the relative intensity of the D (disorder) mode versus the tangential G mode ( $1550\text{--}1600\text{ cm}^{-1}$ ) is often used as a measure of the level of substitution. However, we have shown that Raman is an unreliable method for determination of the extent of functionalization since the relative intensity of the D band is also a function of the substituents' distribution as well as concentration. We have shown that while Raman is useful in demonstrating the presence of  $\text{sp}^3$  carbon atoms within the SWNT sidewall, its use for quantitative analysis is dubious.<sup>6</sup> Thus, it is often difficult to definitively characterize functionalized SWNTs. This state of affairs is in contrast to that of other organic or inorganic molecules (even polymers) where NMR has been successfully used as a primary tool for both compositional and structural characterization.

As would be expected, the low solubility and large size (and hence slow tumbling in solution) limited useful solution NMR studies.<sup>14</sup> Prior solid-state NMR studies have proved useful for the observation of substituents<sup>14b,15–18</sup> but, unfortunately, usually less so with regard to the observation of the important quaternary  $\text{sp}^3$  sidewall carbon atoms<sup>19</sup> that would provide definitive evidence for covalent attachment. In one report, the quaternary sidewall carbon atoms were clearly detected by obtaining cross polarization magic angle spinning (CPMAS) spectra with and without a dephasing delay before FID acquisition.<sup>18</sup> As part of our ongoing studies on the NMR characterization of functionalized SWNTs, we were interested in the study of one of the simplest examples of substituted SWNTs. Our results are presented herein.

## Results and Discussion

HiPCo SWNTs produced at Rice University were purified to remove iron and other impurities<sup>20</sup> and subsequently fluorinated to a C:F ratio of approximately 2.1:1 by direct fluorination at  $150\text{ }^\circ\text{C}$  by a previously reported procedure.<sup>2</sup> The Raman spectra using  $780\text{ nm}$  (red laser) excitation for F-SWNTs show in addition to the tangential G mode (ca.

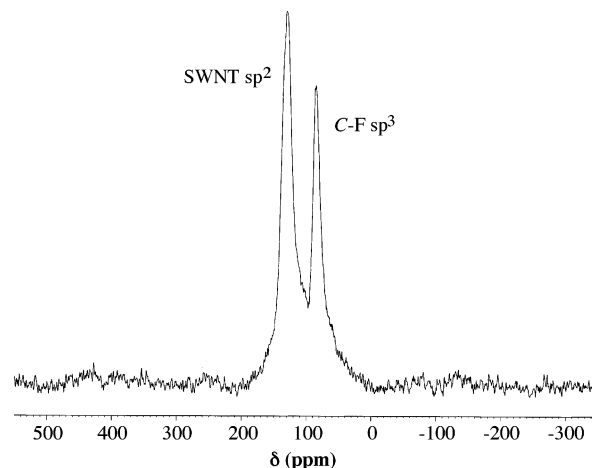


**Figure 1.**  $^{13}\text{C}$  MAS NMR spectrum of F-SWNTs obtained at 50.3 MHz  $^{13}\text{C}$  (4.7 T) and 15 kHz spinning ( $4.5\ \mu\text{s}$   $90^\circ$   $^{13}\text{C}$  pulse, 20.5 ms FID ( $^1\text{H}$  decoupling not used), 10 s relaxation delay, 8600 scans). FID was processed with 50 Hz (1 ppm) of line broadening. Spinning sidebands would be  $\pm 298$  ppm from a center band and clearly are negligible.

$1587\text{ cm}^{-1}$ ) an intense broad D (disorder) mode at ca.  $1295\text{ cm}^{-1}$  consistent with sidewall functionalization.<sup>13</sup>

The 50.3 MHz  $^{13}\text{C}$  MAS NMR spectrum of a sample of F-SWNTs is shown in Figure 1. Chemical shifts are relative to the peak for glycine carbonyl defined as 176.46 ppm.<sup>21</sup> The center band at  $\delta$  128 ppm is typical of the  $\text{sp}^2$  carbon of the sidewall of an SWNT.<sup>17,18,22</sup> The relative areas of the downfield and upfield signals are close to those expected given the C:F ratio determined from X-ray photoelectron spectroscopy (XPS), suggesting an assignment for the upfield signal of  $\text{sp}^3$  carbon atoms attached to fluorine (i.e., CF). Strong support for such an assignment is provided by literature  $^{13}\text{C}$  chemical shift data for relatively simple tertiary alkyl fluorides and fluorinated derivatives of  $\text{C}_{60}$ . With a center band maximum of 83.5 ppm, this signal from the F-SWNTs is about 7–15 ppm upfield of that exhibited by CF in tertiary alkyl fluorides containing 1-fluoroadamantyl,<sup>23</sup> 1-fluorobicyclo[2.2.2]octyl,<sup>24</sup> and 1-fluorobicyclo[3.3.1]nonyl<sup>25</sup> groups and as much as 20 ppm upfield of the signal exhibited by CF in more strained 1-fluorobicyclo[2.2.1]heptyl groups.<sup>26</sup> However, a peak maximum of 83.5 ppm for the F-SWNTs is identical to that reported in the  $^{13}\text{C}\{^{19}\text{F}\}$  spectrum of  $T_h\text{-C}_{60}\text{F}_{24}$ , which has 24 equivalent, isolated CF groups.<sup>27</sup>

Pairs of fluorine atoms would be expected to add to the SWNTs in a 1,2- or 1,4-fashion. Unfortunately, compounds with two or more aliphatic CF groups appear to be rare, thus

- (13) Dresselhaus, M. S.; Pimenta, M. A.; Ecklund, P. C.; Dresselhaus, G. In *Raman Scattering in Materials Science*; Webber, W. H., Merlin, R., Eds.; Springer-Verlag: Berlin, 2000.
- (14) (a) Mickelson, E. T.; Chiang, I. W.; Zimmerman, J. L.; Boul, P. J.; Lozano, J.; Liu, J.; Smalley, R. E.; Hauge, R. H.; Margrave, J. L. *J. Phys. Chem. B* **1999**, *103*, 4318. (b) Kitaygorodskiy, A.; Wang, W.; Xie, S.-Y.; Lin, Y.; Fernando, K. A. S.; Wang, X.; Qu, L.; Chen, B.; Sun, Y.-P. *J. Am. Chem. Soc.* **2005**, *127*, 7517.
- (15) Cahill, L. S.; Yao, Z.; Adronov, A.; Penner, J.; Moonosawmy, K. R.; Kruse, P.; Goward, G. R. *J. Phys. Chem. B* **2004**, *108*, 11412.
- (16) Bac, C. G.; Bernier, P.; Latil, S.; Jourdain, V.; Rubio, A.; Jhang, S. H.; Lee, S. W.; Park, Y. W.; Holzinger, M.; Hirsch, A. *Curr. Appl. Phys.* **2001**, *1*, 149.
- (17) Peng, H.; Alemany, L. B.; Margrave, J. L.; Khabashesku, V. N. *J. Am. Chem. Soc.* **2003**, *125*, 15174.
- (18) Liang, F.; Alemany, L. B.; Beach, J. M.; Billups, W. E. *J. Am. Chem. Soc.* **2005**, *127*, 13941.
- (19) Zhang, L.; Yang, J.; Edwards, C. L.; Alemany, L. B.; Khabashesku, V. N.; Barron, A. R. *Chem. Commun.* **2005**, 3265.
- (20) Chiang, I. W.; Brinson, B. E.; Huang, A. Y.; Willis, P. A.; Bronikowski, M. J.; Margrave, J. L.; Smalley, R. E.; Hauge, R. H. *J. Phys. Chem. B* **2001**, *105*, 8297.

- (21) Hayashi, S.; Hayamizu, K. *Bull. Chem. Soc. Jpn.* **1991**, *64*, 685.
- (22) Hayashi, S.; Hoshi, F.; Ishikura, T.; Yumura, M.; Ohshima, S. *Carbon* **2003**, *41*, 3047.
- (23) (a) Maciel, G. E.; Dorn, H. C.; Greene, R. L.; Kleschick, W. A.; Peterson, M. R., Jr.; Wahl, G. H., Jr. *Org. Magn. Reson.* **1974**, *6*, 178. (b) Olah, G. A.; Shih, J. G.; Singh, B. P.; Gupta, B. G. B. *J. Org. Chem.* **1983**, *48*, 3356.
- (24) (a) Adcock, W.; Abeywickrema, A. N. *J. Org. Chem.* **1982**, *47*, 2957. (b) Adcock, W.; Iyer, V. S. *J. Org. Chem.* **1985**, *50*, 1538.
- (25) Kalinowski, H.-O.; Berger, S.; Braun, S. *Carbon-13 NMR Spectroscopy*; John Wiley & Sons: Chichester, U.K., 1988.
- (26) Adcock, W.; Abeywickrema, A. N.; Kok, G. B. *J. Org. Chem.* **1984**, *49*, 1387.
- (27) Denisenko, N. I.; Troyanov, S. I.; Popov, A. A.; Kuvychko, I. V.; Zemva, B.; Kemnitz, E.; Strauss, S. H.; Boltalina, O. V. *J. Am. Chem. Soc.* **2004**, *126*, 1618.

making it hard to assess the effect of multiple fluorine atoms on the F-SWNT CF  $^{13}\text{C}$  chemical shifts.  $^{13}\text{C}$  NMR data are available for two 1,4-difluoro aliphatic compounds. Replacing the bridgehead H in 1-fluorobicyclo[2.2.2]octane with F (to form 1,4-difluorobicyclo[2.2.2]octane) shields the CF by 3.0 ppm and gives a signal at  $\delta$  91.6.<sup>24a</sup> Replacing the bridgehead H in 9-fluorotriptycene with F (to form 9,10-difluorotriptycene) shields the CF by 1.6 ppm and gives a signal at  $\delta$  97.2.<sup>28</sup> The only 1,2-difluoro compounds of which we are aware with fluorine atoms on adjacent tertiary alkyl carbons are *cis*-15,16-difluoro-15,16-dihydropyrene<sup>29</sup> and  $\text{C}_{2v}\text{-C}_{60}\text{F}_2$ ,<sup>30</sup> both of which would be very good models for 1,2-fluorine addition to an SWNT. Unfortunately,  $^{13}\text{C}$  NMR data were not reported for the pyrene derivative, while the  $^{19}\text{F}$ -coupled  $^{13}\text{C}$  signals for the  $\text{sp}^3$  carbon in 1,2- $\text{C}_{60}\text{F}_2$  were not detected.<sup>30</sup> Multiple fluorination of fullerenes clearly compounds the difficulty of detecting  $^{13}\text{C}$  signals in the absence of fluorine decoupling. For example, no  $^{13}\text{C}$  NMR data were reported for  $D_{5d}\text{-C}_{60}\text{F}_{20}$ , which has a single type of CF group in a  $(\text{CF})_{20}$  loop.<sup>31</sup> However,  $^{13}\text{C}$  signals ranging from  $\delta$  84.0 to  $\delta$  91.2 were tentatively reported for the four different types of CF groups in  $\text{C}_{3v}\text{-C}_{60}\text{F}_{18}$ ,<sup>32</sup>  $^{13}\text{C}$  signals ranging from  $\delta$  86.5 to  $\delta$  91.3 were reported for the three different types of CF groups in the  $(\text{CF})_{15}$  loop of  $\text{C}_{3v}\text{-C}_{60}\text{F}_{15}\{\text{C}[\text{C}(\text{O})\text{OCH}_2\text{CH}_3]_3\}_3$ ,<sup>33</sup> and  $^{13}\text{C}$  signals ranging from  $\delta$  86 to  $\delta$  90 were reported for the CF groups in a mixture of materials analyzing as  $\text{C}_{60}\text{F}_{46}$ .<sup>34</sup> Lacking  $^{13}\text{C}$  NMR data for simple 1,2-difluoro compounds with fluorines on adjacent tertiary alkyl carbons, we note that a fluorine atom usually has a modest deshielding effect on the adjacent  $\beta$ -carbon, i.e., FCC-, compared to the corresponding carbon in an HCC- environment.<sup>35</sup> Thus, the unusually shielded CF  $^{13}\text{C}$  NMR signals observed in the F-SWNTs (Figure 1) may result from the nanotube environment exerting a significant shielding effect. Calculations (see below) are consistent with 1,2-

addition to the SWNTs predominating. From Figure 1 it appears that the  $\text{sp}^2$  signal may be broader than the  $\text{sp}^3$  signal. It is possible this is because the former results from nanotube carbons not near fluorine as well as from those appreciably deshielded carbons adjacent to CF. The unusually shielded  $^{13}\text{C}$  NMR signals observed for the F-SWNTs are not the only interesting anomaly observed for this spectrum. Fluorine-substituted carbons exhibiting different chemical shifts are to be expected because the starting material is a complex mixture of SWNTs differing in diameter and chirality and because fluorination, like alkylation,<sup>18</sup> is expected to occur at different nanotube sites and with the possibility of different addition patterns. Given this expectation, the CF signal is somewhat narrower than expected in comparison with the nanotube  $\text{sp}^2$  carbon signal (Figure 1).

MAS can much more effectively eliminate  $^{13}\text{C}$ - $^{19}\text{F}$  dipole-dipole broadening than  $^{13}\text{C}$ - $^1\text{H}$  dipole-dipole broadening because the dipolar coupling constant has an inverse cube dependence on the C-X bond length (i.e.,  $D_{\text{CF}} \propto 1/r_{\text{CF}}^3$ ) and  $r_{\text{CF}}$  is 0.3 Å longer than  $r_{\text{CH}}$  [e.g.,  $r_{\text{CF}} = 1.383$  Å and  $r_{\text{CH}} = 1.087$  Å in  $\text{CH}_3\text{F}$ ,  $r_{\text{CF}} = 1.43$  Å in  $(\text{CH}_3)_3\text{CF}$ , and  $r_{\text{CH}} = 1.122$  Å in  $(\text{CH}_3)_3\text{C-H}$ ].<sup>36</sup> Furthermore, these data show that  $r_{\text{CF}}$  in a tertiary alkyl fluoride is slightly longer than in less highly substituted fluorides. As a result, compared to  $D_{\text{CH}}$ ,  $D_{\text{CF}}$  is reduced by slightly more than a factor of 2, which significantly aids line narrowing just by MAS. The large influence of the bond length on line narrowing has also been demonstrated with the 4.7 T,  $^{119}\text{Sn}$  MAS NMR spectrum of trimesityltin fluoride,  $[2,4,6\text{-}(\text{CH}_3)_3\text{C}_6\text{H}_2]_3\text{SnF}$ . This compound has  $r_{\text{SnF}} = 1.96$  Å for each molecule in the asymmetric unit, and MAS at just 3.1 kHz clearly gives a pair of  $^1J_{\text{SnF}}$  doublets for the two molecules.<sup>37</sup> To further understand the narrow line width of the CF signal, we have investigated the effect of the spinning speed on the spectral resolution.

$^{13}\text{C}$  spectra obtained on the F-SWNTs with 6, 9, 12, and 15 kHz MAS (the maximum possible with our probe using rotors with an outer diameter of 4 mm) show (Figure 2, left) that increasing the spinning speed from 6 to 9 to 12 kHz causes a steady, significant increase in the signal intensity for the upfield CF signal relative to the downfield nanotube  $\text{sp}^2$  carbon signal, but that only a relatively modest further increase is achieved with 15 kHz MAS. To be sure, the faster spinning also increases the intensity of each center band relative to the intensity of the various spinning sidebands, but it is clear that reducing  $^{13}\text{C}$ - $^{19}\text{F}$  dipole-dipole interactions is much more important than reducing chemical shift anisotropy effects in generating center band signals. Thus, 15 kHz MAS appeared to be rather effective at eliminating the  $^{13}\text{C}$ - $^{19}\text{F}$  dipole-dipole broadening in this sample of highly fluorinated SWNTs, an observation that is particularly encouraging as relatively few laboratories, including our own, have solid-state  $^{19}\text{F}$  capability.

The observation of signals from C-F groups was confirmed by obtaining spectra at 6, 9, 12, 15, 20, 25, and 30

- (28) Adcock, W.; Iyer, V. S. *J. Org. Chem.* **1988**, *53*, 5259.  
 (29) (a) Mitchell, R. H.; Vinod, T. K.; Bodwell, G. J.; Weerawarna, K. S.; Anker, W.; Williams, R. V.; Bushnell, G. W. *Pure Appl. Chem.* **1986**, *58*, 15. (b) Mitchell, R. H.; Bodwell, G. J.; Vinod, T. K.; Weerawarna, K. S. *Tetrahedron Lett.* **1988**, *29*, 3287.  
 (30) Boltalina, O. V.; Lukonin, A. Y.; Street, J. M.; Taylor, R. *Chem. Commun.* **2000**, 1601.  
 (31) (a) Boltalina, O. V.; Markov, V. Y.; Troshin, P. A.; Darwish, A. D.; Street, J. M.; Taylor, R. *Angew. Chem., Int. Ed.* **2001**, *40*, 787. (b) Popov, A. A.; Goryunkov, A. A.; Goldt, I. V.; Kareev, I. E.; Kuvychko, I. V.; Hunnius, W.-D.; Seppelt, K.; Strauss, S. H.; Boltalina, O. V. *J. Phys. Chem. A* **2004**, *108*, 11449.  
 (32) Avent, A. G.; Boltalina, O. V.; Fowler, P. W.; Lukonin, A. Y.; Pavlovich, V. K.; Sandall, J. P. B.; Street, J. M.; Taylor, R. *J. Chem. Soc., Perkin Trans. 2* **1998**, 1319.  
 (33) Burley, G. A.; Avent, A. G.; Goldt, I. V.; Hitchcock, P. B.; Al-Matar, H.; Paolucci, D.; Paolucci, F.; Fowler, P. W.; Soncini, A.; Street, J. M.; Taylor, R. *Org. Biomol. Chem.* **2004**, *2*, 319.  
 (34) Cox, D. M.; Cameron, S. D.; Tuinman, A.; Gakh, A.; Adcock, J. L.; Compton, R. N.; Hagaman, E. W.; Kniaz, K.; Fischer, J. E.; Strongin, R. M.; Cichy, M. A.; Smith, A. B. *J. Am. Chem. Soc.* **1994**, *116*, 1115.  
 (35) Relevant data demonstrating the  $\beta$ -deshielding effect: (a) C-2 in adamantane at  $\delta$  38.4 vs C-2 in 1-fluoroadamantane at  $\delta$  43.4 (see ref 25); (b) C-2 in bicyclo[2.2.1]heptane at  $\delta$  29.6 vs C-2 in 1-fluorobicyclo[2.2.1]heptane at  $\delta$  32.03 (see refs 25 and 26); (c) C-2 in bicyclo[3.3.1]nonane at  $\delta$  32.0 vs C-2 in 1-fluorobicyclo[3.3.1]nonane at  $\delta$  37.3 (see ref 25); (d) C-2 in bicyclo[2.2.2]octane at  $\delta$  25.9 vs C-2 in 1-fluorobicyclo[2.2.2]octane at  $\delta$  31.0 (see ref 25). (e) The only example that we know of with a  $\beta$ -shielding effect: C-8a in triptycene at  $\delta$  144.73 vs C-8a in 9-fluorotriptycene at  $\delta$  143.36 (see ref 28 and Qiu, Z. W.; Grant, D. M.; Pugmire, R. J. *J. Am. Chem. Soc.* **1982**, *104*, 2747).

- (36) (a) Margulès, L.; Demaison, J.; Boggs, J. E. *J. Phys. Chem. A* **1999**, *103*, 7632. (b) Lide, D. R., Jr.; Mann, D. E. *J. Chem. Phys.* **1958**, *29*, 914. (c) Hilderbrandt, R. L.; Wieser, J. D. *J. Mol. Struct.* **1973**, *15*, 27.  
 (37) Bai, H.; Harris, R. K.; Reuter, H. *J. Organomet. Chem.* **1991**, *408*, 167.



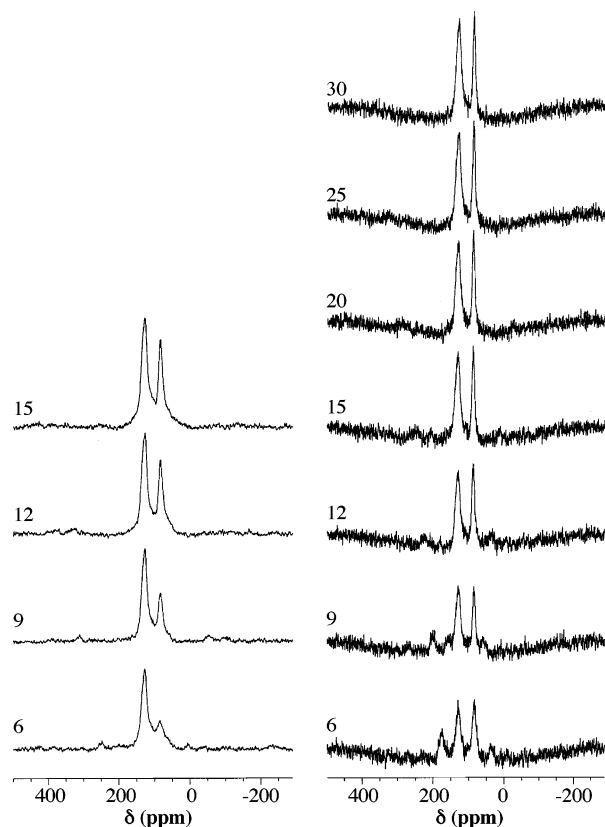


**Figure 2.**  $^{13}\text{C}$  MAS NMR spectra of F-SWNTs obtained at 50.3 MHz  $^{13}\text{C}$  with a 4 mm o.d. rotor (left, 56.9 mg) and at 125.8 MHz  $^{13}\text{C}$  with a 2.5 mm o.d. rotor (right, 5.4 mg) at the spinning speeds indicated (kHz) ( $90^\circ$   $^{13}\text{C}$  pulse (4.5  $\mu\text{s}$  at 50.3 MHz, 2.0  $\mu\text{s}$  at 125.8 MHz), 20.5 ms FID ( $^1\text{H}$  decoupling not used), 10 s relaxation delay, 8600 scans). FID was processed with 50 Hz (1 ppm at 50.3 MHz, 0.4 ppm at 125.8 MHz) of line broadening. Spinning sidebands are clearly evident in the spectra obtained at slower spinning speeds and at the higher field strength.

kHz using a probe on our 500 MHz spectrometer (125.8 MHz  $^{13}\text{C}$ ) designed for 2.5 mm rotors (Figure 2, right). It is clear that increasing the spinning speed from 15 to 30 kHz has relatively little effect, even though chemical shift anisotropy effects are 2.5 times larger on the 500 MHz spectrometer and even though the signal-to-noise ratio is much lower on the 500 MHz spectrometer because the smaller rotor contains 10 times less material. Thus, using 15 kHz MAS with the larger rotor on the 200 MHz spectrometer appears to be adequate for obtaining useful  $^{13}\text{C}$  spectra of F-SWNTs. The spinning sidebands are negligible and the signal-to-noise ratio is much higher compared to those of the corresponding spectrum obtained on the 500 MHz spectrometer, although the center band nanotube  $\text{sp}^2$  signal and center band C–F signal are not as well resolved at the lower field. In studies of polymers, others have also observed the beneficial effect of fast MAS for generating  $^{13}\text{C}$  signals by attenuating strong  $^{13}\text{C}$ – $^{19}\text{F}$  dipole–dipole interactions.<sup>38</sup>

Intramolecular dipole–dipole interactions can also be effectively averaged by rapid molecular tumbling in nearly spherical molecules possessing high symmetry. Adamantane is perhaps the best known such example. Relatively slow (2.2 kHz) MAS without proton decoupling significantly

narrows its  $^{13}\text{C}$  signals.<sup>39</sup> In this context, it is worth noting that  $D_3$ - and  $S_6$ - $\text{C}_{60}\text{F}_{48}$ , which are nearly spherical isomers,<sup>40</sup> give a 75.5 MHz  $^{13}\text{C}$  MAS spectrum with at least six partially resolved CF signals ranging from 83 to 96 ppm with MAS at just 2.84 kHz.<sup>41</sup> Each of these isomers of  $\text{C}_{60}\text{F}_{48}$  has eight different CF environments (with C–F bond lengths ranging from 1.358 to 1.395 Å in the  $D_3$  isomer).<sup>40</sup> The  $D_3$  and  $S_6$  isomers consist of two equivalent hemispheres related by  $C_2$  rotation or inversion, respectively.<sup>40</sup> The authors attribute the complexity of the CF region of the  $^{13}\text{C}$  MAS spectrum to  $^{13}\text{C}$ – $^{19}\text{F}$  scalar coupling. In any event, what is noteworthy is the ability to detect CF signals in  $\text{C}_{60}\text{F}_{48}$  just with relatively slow MAS. With respect to shape, long, highly anisotropic F-SWNTs are the opposite of nearly spherical  $\text{C}_{60}\text{F}_{48}$ , and faster MAS is accordingly required for generating relatively sharp CF signals from F-SWNTs.

We should note that the observed  $^{13}\text{C}$  NMR signals in the spectra of the F-SWNTs result entirely from the F-SWNTs, as no  $^{13}\text{C}$  signal is detected on the 200 MHz spectrometer under the same conditions when an empty rotor (zirconia rotor barrel and Kel-F cap) is spun at 15 kHz. Kel-F, which is poly(chlorotrifluoroethylene), under suitable spectroscopic conditions gives  $^{13}\text{C}$  signals at 115 and 104 ppm for the  $\text{CF}_2$  and  $\text{CFCl}$  groups.<sup>38,42</sup> Similarly, the  $^{13}\text{C}$  signals observed on the 500 MHz spectrometer result entirely from the F-SWNTs, as they are not detected when a fluorine-free empty rotor (zirconia rotor barrel and Vespel end caps) is used.

Unfortunately,  $^{13}\text{C}$  MAS NMR of F-SWNTs does not clearly indicate whether any  $\text{CF}_2$  groups were generated by C–C bond cleavage and fluorination, as the signals for  $\text{CF}_2$  groups and nanotube  $\text{sp}^2$  carbons would be expected to overlap significantly.<sup>38,43,44</sup> XPS does indicate the presence of  $\text{CF}_2$  groups in this sample of F-SWNTs. Clearly, it would be desirable to be able to decouple  $^{19}\text{F}$  both by magic angle spinning and by applying rf pulse sequences<sup>38,44,45</sup> to determine whether the downfield  $^{13}\text{C}$  signal changes when pulsed  $^{19}\text{F}$  decoupling is used. A  $^{13}\text{C}$  spectrum obtained with the phases of the signals modulated by the scalar  $^{13}\text{C}$ – $^{19}\text{F}$  couplings<sup>38</sup> will not differentiate nanotube  $\text{sp}^2$  carbon from  $\text{CF}_2$ , as both types of signals will have the same phase. In another approach, trying to unambiguously detect a low level of  $\text{CF}_2$  groups in the presence of a large amount of nanotube  $\text{sp}^2$  carbons in a  $^{13}\text{C}$ – $^{19}\text{F}$  dipolar dephasing experiment<sup>45</sup> would clearly be difficult, not only because the  $\text{CF}_2$  groups are a minor component, but also because the signal for nanotube  $\text{sp}^2$  carbons adjacent to the  $\text{CF}_2$  groups would be expected to be attenuated as well, albeit to a smaller extent. Conversely, a  $^{19}\text{F}$ – $^{13}\text{C}$  CPMAS experiment would preferentially detect the  $\text{CF}_2$  groups, but nanotube  $\text{sp}^2$  carbons

(39) Stejskal, E. O.; Schaefer, J.; Waugh, J. S. *J. Magn. Reson.* **1977**, *28*, 105.

(40) Troyanov, S. I.; Troshin, P. A.; Boltalina, O. V.; Ioffe, I. N.; Sidorov, L. N.; Kemnitz, E. *Angew. Chem., Int. Ed.* **2001**, *40*, 2285.

(41) Privalov, V. I.; Boltalina, O. V.; Galeva, N. A.; Taylor, R. *Dokl. Phys. Chem.* **1998**, *360*, 182.

(42) Fleming, W. W.; Fyfe, C. A.; Lyster, J. R.; Vanni, H.; Yannoni, C. S. *Macromolecules* **1980**, *13*, 460.

(43) Grinstead, R. A.; Koenig, J. L. *J. Polym. Sci., Part B: Polym. Phys.* **1990**, *28*, 177.

(44) Holstein, P.; Scheler, U.; Harris, R. K. *Magn. Reson. Chem.* **1997**, *35*, 647.

(45) Hagaman, E. W. *J. Magn. Reson., A* **1993**, *104*, 125.

(38) Liu, S.-F.; Schmidt-Rohr, K. *Macromolecules* **2001**, *34*, 8416.

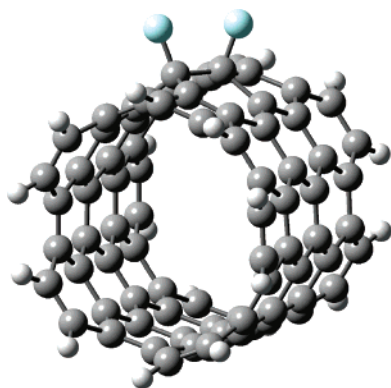


**Figure 3.** Calculated structure of the 5,5-SWNT  $\text{C}_{80}\text{H}_{20}$  fragment with two fluorine atoms (1,2-addition).

adjacent to  $\text{CF}_2$  groups should also be detected.  $^{19}\text{F}$  MAS NMR might be useful for detecting  $\text{CF}_2$  groups in the presence of CF groups—provided that  $^{19}\text{F}$ – $^{19}\text{F}$  and (if present)  $^{19}\text{F}$ – $^1\text{H}$  dipole–dipole interactions can be effectively averaged—as  $\text{CF}_2$  groups appear to be considerably more deshielded than tertiary alkyl CF groups.<sup>28,46</sup>

With the peak at 83.5 ppm confidently assigned to the  $\text{sp}^3$  CF carbon atoms, two questions arise. First, can it be assigned to either 1,2- or 1,4-addition of the fluorine to the SWNT sidewall? Second, with the peak due to CF, why is there no scalar  $^{13}\text{C}$ – $^{19}\text{F}$  coupling observed?

To determine whether the observed peaks could be assigned to either 1,2- or 1,4-addition, the theoretical  $^{13}\text{C}$  NMR shifts have also been calculated for a series of substituted F-SWNT fragments. To simplify the calculations, a  $\text{C}_{80}\text{H}_{20}$  fragment of the 5,5 (armchair) conformation was used (e.g., Figure 3). The calculated shifts for the  $\text{sp}^3$  (CF) and  $\text{sp}^2$  carbons are shown in Figure 4 for single and double 1,2- and 1,4-addition to the SWNT sidewall. As may be seen from Figure 4 the experimentally observed spectrum of F-SWNTs (84 ppm) is consistent with multiple 1,2-additions (ca. 82 ppm). Given the line width for the spectrum (Figure 1), the calculations do not preclude the presence of a minor component of 1,4-addition products; however, we propose that F-SWNTs are predominantly those of 1,2-addition products as proposed by Scuseria and co-workers.<sup>8</sup>

On the basis of the model compound data and the calculated  $^{13}\text{C}$  NMR shifts, the peak at 84 ppm is undoubtedly due to the  $\text{sp}^3$  carbon atoms; however, this begs a second question as to why no scalar  $^{13}\text{C}$ – $^{19}\text{F}$  coupling is observed. Isotropic  $J$  couplings are unaffected by MAS,<sup>47</sup> and thus, one might at first expect to observe  $^{13}\text{C}$ – $^{19}\text{F}$   $J$  couplings, which are typically about 180–210 Hz in tertiary alkyl fluorides.<sup>23a,24,26–28</sup> However, such couplings are not observed in the  $^{13}\text{C}$  spectra of the F-SWNTs. Three explanations, all of which probably apply, can be proposed. First, with fluorine-substituted  $^{13}\text{C}$  nuclei present in different environments, numerous  $^1J_{\text{CF}}$  doublets could overlap, thus obscuring any fine structure.  $^1J_{\text{CF}}$  values in F-SWNTs generated by

multiple 1,2-additions may also be larger than  $^1J_{\text{CF}}$  values in monofluoro tertiary alkyl fluorides.  $\text{C}_{60}\text{F}_{15}\{\text{C}[\text{C}(\text{O})\text{OCH}_2\text{CH}_3]_3\}_3$  contains a  $(\text{CF})_{15}$  loop with three different types of CF groups that exhibit  $^1J_{\text{CF}}$  values  $\sim 240$  Hz.<sup>33</sup> In addition, two-, three-, and four-bond  $J_{\text{CF}}$  couplings expected to range from about 25 to 1 Hz would further broaden the observed  $^{13}\text{C}$  signal.<sup>23a,24,26,28,33</sup>

A probably more significant reason for not observing  $^{13}\text{C}$ – $^{19}\text{F}$   $J$  couplings is that, at finite MAS speeds, the cross term in the first-order average Hamiltonian between the homonuclear  $^{19}\text{F}$ – $^{19}\text{F}$  dipolar coupling and the heteronuclear  $^{13}\text{C}$ – $^{19}\text{F}$  dipolar coupling leads to a direct broadening of the  $^{13}\text{C}$  resonances.<sup>47</sup> In addition, magnetization exchange between the doublet components caused by the fluorine spin diffusion process manifests itself in the  $^{13}\text{C}$  spectrum like a chemical exchange process, i.e., the two  $^{13}\text{C}$  signals of a  $^{13}\text{C}$ – $^{19}\text{F}$  doublet can collapse into a singlet (a self-decoupling of the  $J$  interaction) whose line width depends on the MAS speed.<sup>47,48</sup> If the fluorine spin diffusion rate is much smaller than  $J$ , a well-resolved doublet may be observed.<sup>48</sup> This appears to be the case in the  $^{119}\text{Sn}$  MAS spectrum of trimesityltin fluoride (see above), where the  $^{19}\text{F}$ – $^{19}\text{F}$  separation is 6.42 Å.<sup>37</sup> An intermediate situation (a severely broadened doublet) has been reported for the  $^{13}\text{C}$ – $^{19}\text{F}$  spin pair in (2-fluorophenyl)glycine.<sup>46</sup> In the limit of a very lightly fluorinated SWNT in which  $^{19}\text{F}$ – $^{19}\text{F}$  dipole–dipole interactions are very weak and the  $^{19}\text{F}$ – $^{19}\text{F}$  spin diffusion rate is much smaller than  $^1J_{\text{CF}}$ , the  $^{13}\text{C}$ – $^{19}\text{F}$  signals might exhibit a detectable  $^1J$  coupling under fast MAS conditions, provided, of course, that these  $^{13}\text{C}$  signals could be detected (see below).  $(\text{CD}_3)_3^{15}\text{N}\cdot\text{HCl}$  provides an analogous situation with  $^{15}\text{N}$  and  $^1\text{H}$  instead of  $^{13}\text{C}$  and  $^{19}\text{F}$ ; in the  $^{15}\text{N}$  spectrum obtained with 30 kHz MAS and no  $^1\text{H}$  decoupling, a sharp doublet resulting from  $^1J_{\text{NH}} \approx 100$  Hz is clearly detected.<sup>49</sup>

**Thermal Decomposition of F-SWNTs.** The ability to quantify the presence of sidewall functionalization by  $^{13}\text{C}$  MAS NMR provides the potential for studying subsequent reactivity of F-SWNTs. One of the simplest reactions of F-SWNTs is their thermal decomposition and the reformation of pristine SWNTs, albeit with the reduction in the length of the SWNTs. F-SWNTs studied in this work decompose between 250 and 600 °C with the loss of  $\text{F}_2$  and fluorine-containing products. F-SWNTs heated to 400, 450, and 550 °C (see the Experimental Section) have been analyzed by  $^{13}\text{C}$  MAS NMR, Raman, and IR spectroscopy and XPS.

Figure 5 shows the  $^{13}\text{C}$  MAS NMR spectra of F-SWNTs at various stages of thermolysis. It is clear that as thermolysis continues the CF groups are removed. In particular the spectra are significantly altered between 400 and 450 °C with a decrease in the size of the peak due to the CF  $\text{sp}^3$  carbons (Table 1). After thermolysis at 550 °C the  $^{13}\text{C}$  MAS NMR spectrum is essentially identical to that of pristine SWNTs, although XPS indicates the presence of a formula of  $\text{C}_{14.1}\text{F}$  (see Table 1), suggesting that the detection of the sidewall-

(46) (a) Weigert, F. J. *J. Org. Chem.* **1980**, *45*, 3476. (b) Carss, S. A.; Scheler, U.; Harris, R. K.; Holstein, P.; Fletton, R. A. *Magn. Reson. Chem.* **1996**, *34*, 63. (c) Scheler, U. *Solid State Nucl. Magn. Reson.* **1998**, *12*, 9.

(47) Ernst, M.; Samoson, A.; Meier, B. H. *Chem. Phys. Lett.* **2001**, *348*, 293.

(48) Ernst, M.; Verhoeven, A.; Meier, B. H. *J. Magn. Reson.* **1998**, *130*, 176.

(49) Ernst, M.; Zimmermann, H.; Meier, B. H. *Chem. Phys. Lett.* **2000**, *317*, 581.

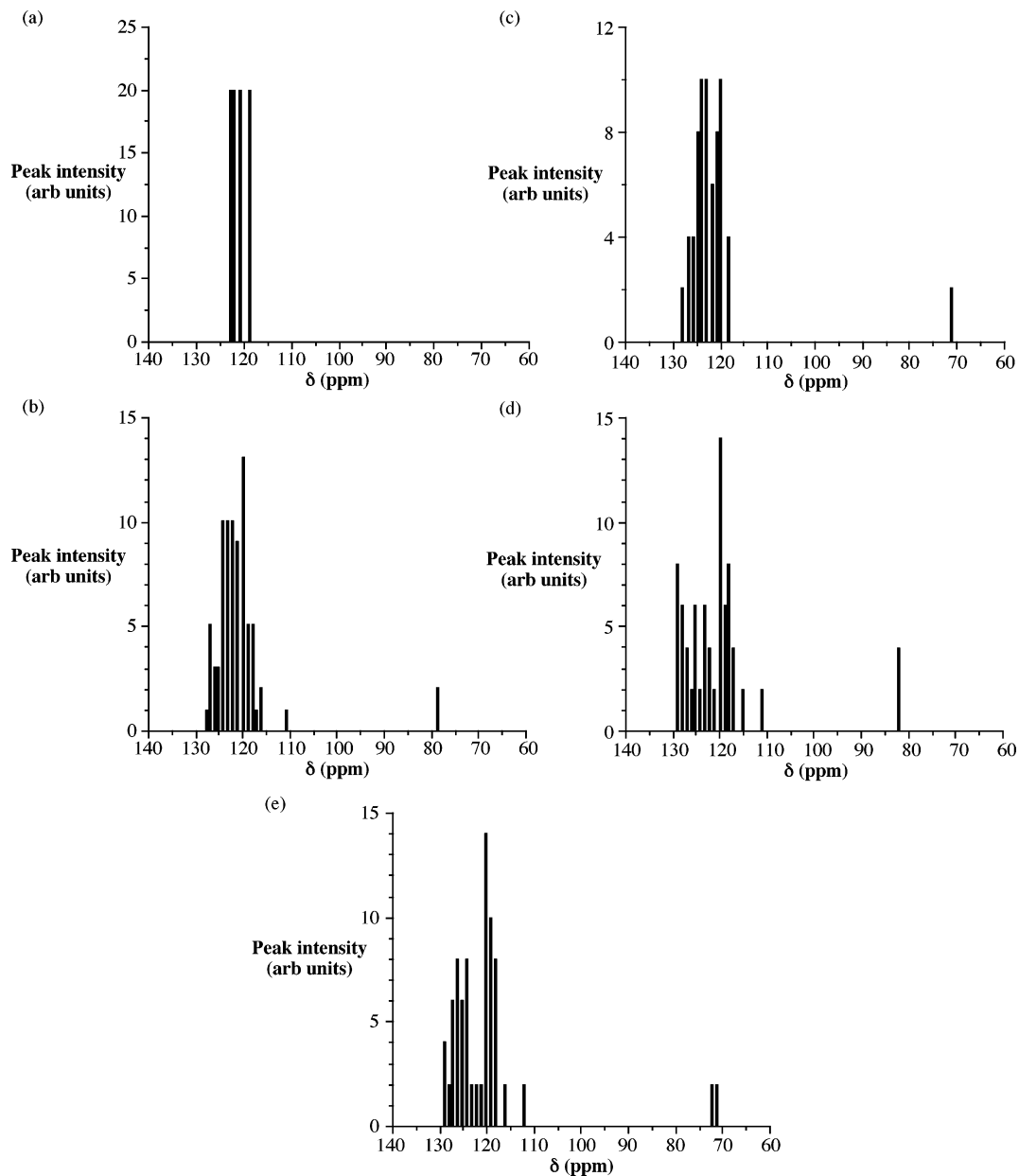


**Figure 4.** Calculated  $^{13}\text{C}$  NMR shifts for (a) the  $\text{C}_{80}\text{H}_{20}$  fragment of the 5,5 (armchair) conformation and as a result of (b) 1,2-addition by two fluorine atoms, (c) 1,4-addition by two fluorine atoms, (d) 1,2-addition by four fluorine atoms, and (e) 1,4-addition by four fluorine atoms.

functionalized  $\text{sp}^3$  carbon is difficult at low levels of functionalization. As fluorine is removed, the peak maximum for the downfield signal shifts upfield, slightly at first (from  $\delta$  128.2 to  $\delta$  126.8 upon heating to 400 °C) and then more noticeably as larger amounts of fluorine are removed (to  $\delta$  123.4 upon heating to 450 °C and to  $\delta$  117.3 upon heating to 550 °C). Thus, fluorine appears to exert the usual  $\beta$ -deshielding effect on nanotube  $\text{sp}^2$  carbons.

As may be seen from Figure 6, the intensity of the D (disorder) band decreases as the thermolysis temperature increases (Table 1). This is consistent with the loss of sidewall functionalization, i.e., fluorine. The G band shows a concomitant sharpening and increase in intensity.<sup>50</sup> In a similar manner, the IR spectrum shows (Supporting Information) a loss of the C–F stretch at 1100  $\text{cm}^{-1}$ .

As expected XPS analysis shows a decrease in F content with increased temperature (Table 1). Furthermore, as has been previously observed, high-resolution C1s and F1s XPS spectra allow for the observation of both CF and  $\text{CF}_2$  moieties (Figures 7 and 8).<sup>10b,51–54</sup> From XPS it appears that the  $\text{CF}_2$  fragments (691.2 eV) are eliminated by thermolysis of F-SWNTs between 400 and 450 °C. It has been proposed that the presence of  $\text{CF}_2$  is associated with cutting sites.<sup>11,12</sup> Thus, our results suggest that the defects are removed prior to the removal of the majority of sidewall CF. This would suggest that the cutting of F-SWNTs is completed by 450

(50) Note the presence of the small band ( $\text{G}^-$ ) to lower wavenumber in the SWNTs heated to 550 °C: Jishi, R. A.; Venkataraman, L.; Dresselhaus, M. S.; Dresselhaus, G. *Phys. Rev. B* **1995**, *51*, 11176.

(51) Lee, Y. S.; Cho, T. H.; Lee, B. K.; Rho, J. S.; An, K. H.; Lee, Y. H. *J. Fluorine Chem.* **2003**, *120*, 99.

(52) Wang, Y.-Q.; Sherwood, P. M. A. *Chem. Mater.* **2004**, *16*, 5427.

(53) Marcoux, P. R.; Schreiber, J.; Batail, P.; Lefrant, S.; Renouard, J.; Jacob, G.; Alberini, D.; Mevellec, J.-Y. *Phys. Chem. Chem. Phys.* **2002**, *4*, 2278.

(54) (a) Kawasaki, S.; Komatsu, K.; Okino, F.; Touhara, H.; Kataura, H. *Phys. Chem. Chem. Phys.* **2004**, *6*, 1769. (b) Shofner, M. L.; Khabashesku, V. N.; Barrera, E. V. *Chem. Mater.* **2006**, *18*, 906.

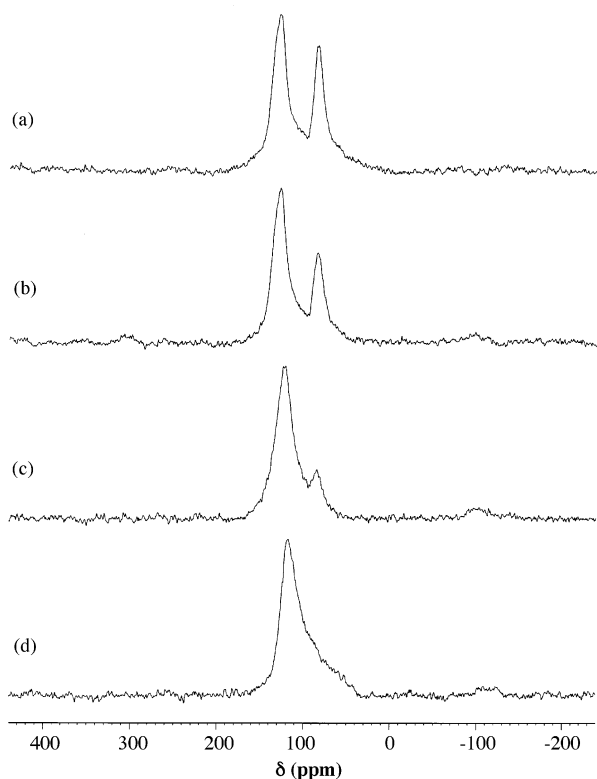


**Figure 5.**  $^{13}\text{C}$  MAS NMR spectra of F-SWNTs obtained at 50.3 MHz  $^{13}\text{C}$  (a) as prepared at 150 °C (parameters as in Figure 1) after heating to (b) 400, (c) 450, and (d) 550 °C, with 11 kHz MAS used for the heated samples (other parameters as in Figure 1).

**Table 1. Analysis of F-SWNTs as a Function of the Thermolysis Temperature**

temp (°C)	XPS C:F ratio	Raman G:D ratio	NMR $\text{sp}^2:\text{sp}^3$ ratio <sup>b</sup>
150 <sup>a</sup>	2.1	0.51	2.3
400	2.4	0.53	4.9
450	4.24	0.54	16
550	14.1	1.50	<sup>c</sup>

<sup>a</sup> As prepared F-SWNTs; see the Experimental Section. <sup>b</sup> The NMR ratios are only approximate in light of the substantial overlap of the  $\text{sp}^2$  carbon and CF signals and the absence of information on the relative relaxation rates of these two types of carbons. <sup>c</sup> Not measurable.

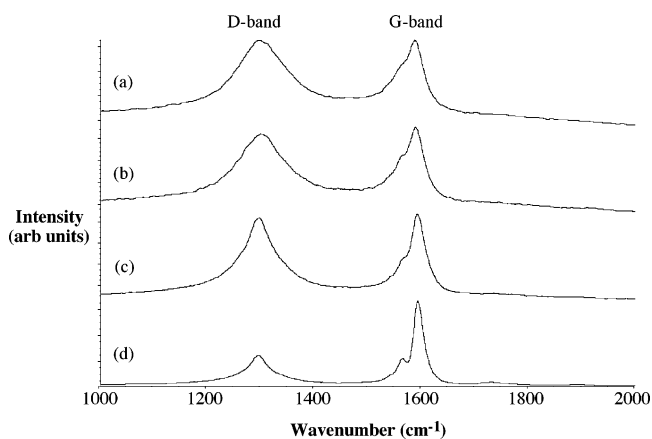


**Figure 6.** Raman spectra of F-SWNTs (a) as prepared at 150 °C and after heating to (b) 400, (c) 450, and (d) 550 °C.

°C, while the removal of sidewall fluorine continues until 600 °C.

In addition to the observation of multiple fluorine species (where  $^{13}\text{C}$  NMR can only distinguish the CF unit), the high-

resolution C1s spectra allow for two types of SWNT  $\text{sp}^2$  carbon. A peak at 284.3–284.8 eV is due to a “normal” SWNT sidewall  $\text{sp}^2$  carbon, while a peak at 285.5 eV can be assigned as being a next-nearest-neighbor  $\text{sp}^2$  carbon (i.e., CCF).<sup>34</sup> Unfortunately, quantification is complicated by the presence of a component in the peak at 285.5 eV due to oxidation defects in the SWNT.<sup>51</sup> Taking these defects into account, a qualitative measurement can be obtained for the relative abundance of CF, CCF, and “normal”  $\text{sp}^2$  carbon atoms as a function of thermolysis temperature (Figure 9). F-SWNTs have been reported to have a bandlike structure, and the concurrent loss of CF and CCF is in agreement with the retention of bands during defluorination.

**NMR versus Raman for Functional Group Quantification.** As noted in the Introduction, the presence of a significant D (disorder) mode has been the primary method for determining the presence of sidewall functionalization.<sup>13</sup> It has been commonly accepted that the relative intensity of the D mode versus the tangential G mode is a measure of the level of substitution. However, we have demonstrated that the G:D ratio is also dependent on the distribution of the substituents. NMR spectroscopy should not show a dependence on the distribution of substituents if the peaks due to the sidewall  $\text{sp}^2$  and  $\text{sp}^3$  carbons can be differentiated.

F-SWNTs offer a nearly ideal system for the study of different spectroscopic techniques for both the confirmation and quantification of sidewall functional groups on SWNTs. First, covalent functionalization is well accepted and has been demonstrated by STM. Second, the substituent contains no carbon, allowing for easy quantification by XPS to provide a reference analytical methodology. Finally, an individual sample of SWNTs can be prepared with a range of substituent concentrations by defluorinating the same batch of F-SWNTs at different temperatures.

Table 1 summarizes the changes in the C:F ratio (XPS), the G:D ratio (Raman), and the ratio of  $\text{sp}^2$  to  $\text{sp}^3$  carbon atoms (NMR). The XPS, Raman, and NMR data demonstrate the same trend consistent with decreasing substituent (F) content as the thermolysis temperature is increased. Figure 10 shows a plot of NMR and Raman analysis as a function of the C:F ratio to ascertain the validity of using these techniques for quantification.<sup>55</sup> The extent of functionalization as measured by  $^{13}\text{C}$  MAS NMR spectroscopy ( $\text{sp}^2:\text{sp}^3$  ratio) shows a direct linear correlation with the F concentration. Unfortunately, in the present case problems in peak integration at low levels of functionalization limit the correlation to high levels of functionalization. In contrast, the use of Raman spectroscopy to quantify the presence of fluorine substituents is clearly suspect. From Figure 10 it appears that there is essentially no change in the G band:D band ratio despite a doubling of the amount of functional group.

(55) It should be noted that even in the present, relatively simple, system while XPS can be used for accurate determination of the C:F ratio, determination of different chemical species (i.e., CF versus CCF) requires fitting of the spectra as described in the text. The presence of multiple overlapping peaks potentially fitted makes quantification somewhat difficult. It is for this reason that XPS can be used for determination of the C:F ratio for comparison with Raman and NMR.



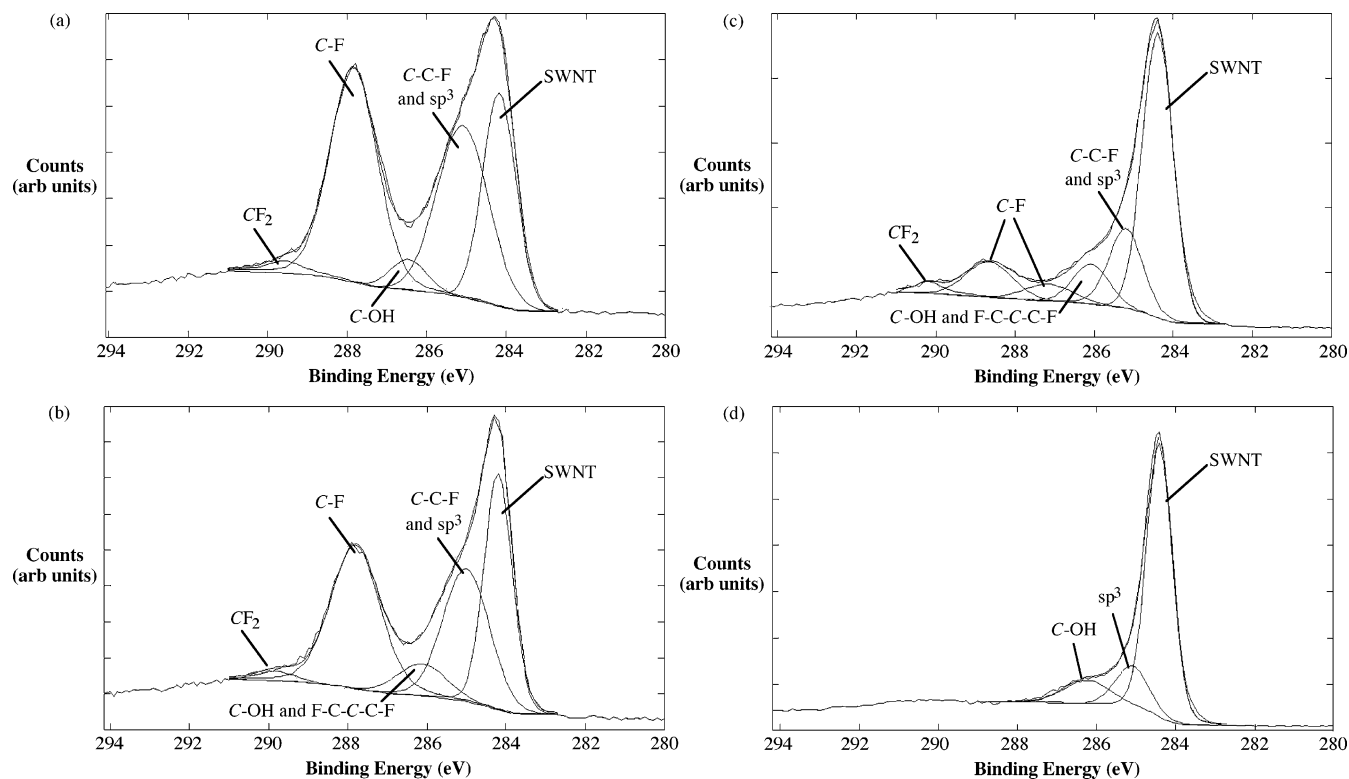


**Figure 7.** C1s high-resolution XPS spectra for F-SWNTs (a) as prepared at 150 °C and after heating to (b) 400, (c) 450, and (d) 550 °C.

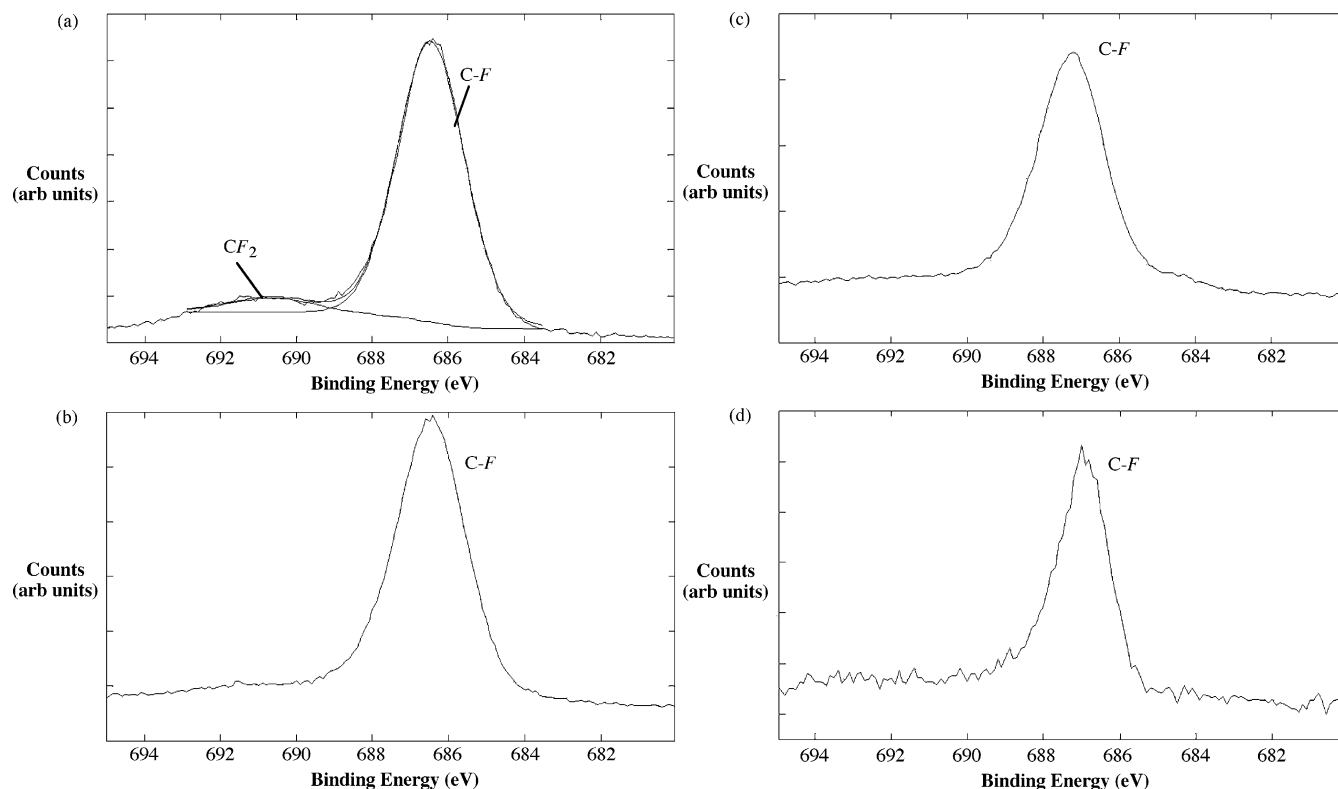


**Figure 8.** F1s high-resolution XPS spectra for F-SWNTs (a) as prepared at 150 °C and after heating to (b) 400, (c) 450, and (d) 550 °C.

On the basis of the data above, we propose that <sup>13</sup>C NMR spectroscopy is best applied for looking at small changes in functionalization at high levels of functionalization. In contrast, Raman spectroscopy, and the relative intensity of the G and D bands, does not provide an accurate quantification of small differences at high levels of functionalization. This is in agreement with our previous studies that Raman

gave misleading results with regard to quantification because of the importance of substituent distribution in determining the intensity of the D band. However, Raman does allow for quantification of large changes in the extent of functionalization. Due to problems in peak integration at low levels of functionalization, NMR is limited more than Raman at low functionalization levels. Such problems may be over-

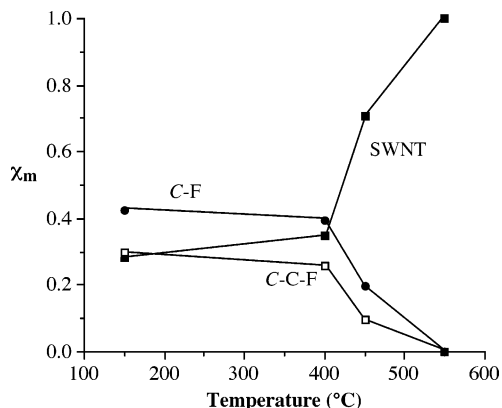


**Figure 9.** Relative amounts of CF (●), CCF (□), and SWNT  $\text{sp}^2$  sidewall carbon atoms (■) as a function of the treatment temperature.

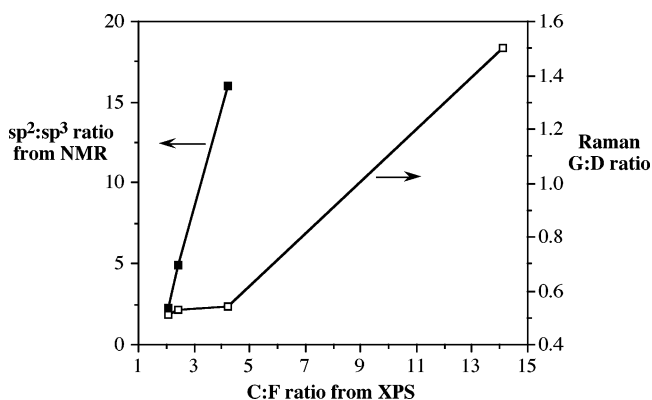


**Figure 10.**  $\text{C}(\text{sp}^2):\text{C-F}(\text{sp}^3)$  ratio (■) and Raman G band:D band ratio (□) as a function of the C:F ratio from XPS.

come to a degree by the use of larger samples. We propose, therefore, that where a comparison of samples with a high degree of functionalization is required NMR provides a much better quantification than Raman. However, where a comparison between samples with low levels of functionalization or large differences in degree of functionalization is required Raman provides a much better quantification than NMR.

## Conclusions

F-SWNTs have been characterized by MAS  $^{13}\text{C}$  NMR spectroscopy and the results correlated with Raman, IR, and X-ray photoelectron spectroscopy measurements. The  $^{13}\text{C}$  NMR shift for the  $\text{sp}^3$  fluorine-substituted (CF) carbon atoms of the SWNT sidewall is observed at 83.5 ppm. This apparently unusual shift is confirmed to be due to the CF moieties from ab initio calculations on a  $\text{C}_{80}$  fragment of the 5,5 (armchair) SWNT and provides the first experimental evidence for the predominance of 1,2-addition rather than 1,4-addition of fluorine. The lack of  $J(^{13}\text{C}-^{19}\text{F})$  coupling for the C-F carbon peak apparently results from interaction between  $^{19}\text{F}-^{19}\text{F}$  and  $^{13}\text{C}-^{19}\text{F}$  dipolar couplings and from magnetization exchange between the  $^{13}\text{C}$  doublet components caused by fluorine spin diffusion. NMR clearly provides a suitable method for demonstrating covalent sidewall functionalization of SWNTs. With regard to the quantification of substituents, we can conclude that  $^{13}\text{C}$  NMR spectroscopy is best applied for looking at small changes in functionalization at high levels of functionalization. We have also shown that, in agreement with our prior results, Raman

spectroscopy should be used cautiously for the quantification of the number of sidewall substituents.

## Experimental Section

HiPCo SWNTs produced at Rice University were purified to remove iron and other impurities using a modification of the literature methods.<sup>20</sup> HiPCo SWNTs were heated at 225 °C in a gas flow of 5%  $\text{O}_2/\text{Ar}$  in a quartz tube furnace for 22 h. The sample was then sonicated in concentrated HCl for 4 h. The color turned to yellow-green as an indication of the presence of  $\text{Fe}^{3+}$  in the solution. The solution pH was adjusted with a double volume of DI water to get iron in solution. The sample was vacuum filtered through a 0.2  $\mu\text{m}$  Cole Palmer Teflon membrane and washed several times with water and ethanol to ensure complete removal of the remaining iron and HCl. After that, the sample was dried in a vacuum oven overnight. XPS results showed that, after purification, there is no presence of the iron catalyst. The purified SWNTs were fluorinated to a C:F ratio of approximately 2.1:1 by direct fluorination at 150 °C by a previously reported procedure.<sup>1</sup> All chemicals were obtained commercially (Aldrich) and were used without any further purification. All water was ultrapure (UP), obtained from a Millipore Milli-Q UV water filtration system. Solutions were filtered using Millipore Express PLUS membranes made of poly(ether sulfone) with 0.22 and 0.1  $\mu\text{m}$  pore sizes. XPS spectra were acquired on a PHI 5700 ESCA system (Physical Electronics) at 15 kV, using an aluminum target and an 800  $\mu\text{m}$  aperture. Samples were pressed into indium metal. Spectra were fitted to the least number of peaks. Peak assignments were based on previously published results.<sup>51-54</sup> Raman spectroscopy on solids (both 785 and 532 nm excitation) was performed using a Renishaw Raman microscope. Samples were mounted on double-stick tape. Attenuated total reflectance infrared spectroscopy (ATR-IR; 4000–600  $\text{cm}^{-1}$ ) of solids was obtained using a Nicolet Nexus 670 FT-IR spectrometer with a diamond window. Thermal analysis was performed on a TA Instruments SDT 2960 using platinum pans.  $^{13}\text{C}$  MAS NMR spectra were obtained with Bruker 200 and 500 MHz spectrometers.<sup>17,18</sup>

The preparation of F-SWNTs after 400 °C heating was performed as follows. Before heating, the reaction vessel that holds 100 mg of F-SWNTs was purged with argon for 30 min at room temperature. Then, under an argon atmosphere, the F-SWNTs were heated to 400 °C and kept at 400 °C for 30 min. The sample was cooled to room temperature. The preparations of F-SWNTs after 450 and 550 °C heating were performed in an analogous manner.

Calculations on the  $\text{C}_{80}\text{H}_{20}$  and subsequent fluorinated fragments were carried out using the Gaussian 03, revision C.02 (Windows version), suite of programs.<sup>56</sup> The geometry optimization was performed by HF/STO-3G, and the NMR calculation was performed

(56) Frisch, M. J.; Trucks, G. W.; Schlegel, H. B.; Scuseria, G. E.; Robb, M. A.; Cheeseman, J. R.; Montgomery, J. A., Jr.; Vreven, T.; Kudin, K. N.; Burant, J. C.; Millam, J. M.; Iyengar, S. S.; Tomasi, J.; Barone, V.; Mennucci, B.; Cossi, M.; Scalmani, G.; Rega, N.; Petersson, G. A.; Nakatsuji, H.; Hada, M.; Ehara, M.; Toyota, K.; Fukuda, R.; Hasegawa, J.; Ishida, M.; Nakajima, T.; Honda, Y.; Kitao, O.; Nakai, H.; Klene, M.; Li, X.; Knox, J. E.; Hratchian, H. P.; Cross, J. B.; Bakken, V.; Adamo, C.; Jaramillo, J.; Gomperts, R.; Stratmann, R. E.; Yazyev, O.; Austin, A. J.; Cammi, R.; Pomelli, C.; Ochterski, J. W.; Ayala, P. Y.; Morokuma, K.; Voth, G. A.; Salvador, P.; Dannenberg, J. J.; Zakrzewski, V. G.; Dapprich, S.; Daniels, A. D.; Strain, M. C.; Farkas, O.; Malick, D. K.; Rabuck, A. D.; Raghavachari, K.; Foresman, J. B.; Ortiz, J. V.; Cui, Q.; Baboul, A. G.; Clifford, S.; Cioslowski, J.; Stefanov, B. B.; Liu, G.; Liashenko, A.; Piskorz, P.; Komaromi, I.; Martin, R. L.; Fox, D. J.; Keith, T.; Al-Laham, M. A.; Peng, C. Y.; Nanayakkara, A.; Challacombe, M.; Gill, P. M. W.; Johnson, B.; Chen, W.; Wong, M. W.; Gonzalez, C.; Pople, J. A., Gaussian, Inc., Wallingford, CT, 2004.

by HF/3-21G. To determine the NMR shift values, the NMR shielding tensor of SiMe<sub>4</sub> was calculated since SiMe<sub>4</sub> is the standard used in the actual NMR experiments. The NMR shielding tensors of the model molecules were then calculated. The difference between the carbon magnetic shielding in SiMe<sub>4</sub> and the carbon magnetic shielding in the model molecule was the calculated NMR value of the carbon in the model molecule.

**Acknowledgment.** Financial support for this work was provided by the Robert A. Welch Foundation. Funds toward

the purchase of the 200 and 500 MHz NMR spectrometers were provided by the Office of Naval Research and the National Science Foundation, respectively.

**Supporting Information Available:** Background XPS data and IR spectra of the F-SWNTs before and after heating (PDF). This material is available free of charge via the Internet at <http://pubs.acs.org>.

CM0618906